BULLETIN OF THE POLISH ACADEMY OF SCIENCES
TECHNICAL SCIENCES,
DOI: 10.24425/bpasts.2025.154207

EMF Signature Analysis in a Marine-Type Brushless Synchronous Generator for Online Fault Detection

Filip Kutt[1]*, **Michał Michna**[1]**, **Grzegorz Kostro**[1]***

[1] Gdansk University of Technology

Abstract. The objective of the paper is to investigate the application of the current signature analysis type approach for the online diagnosis of a marine-type Brushless Synchronous Generator (BSG). The system's diagnostic would be done using an automated test procedure when the generator comes online or offline. The analysis of the measured electromotive force waveform (EMF) is used for fault detection. The paper's main contribution is the development of a fault detection algorithm that would allow the generator to be safely operated in remote marine-type conditions where low maintenance costs are a crucial aspect of the system operation. To verify the diagnostic algorithm, a special measurement system was developed to emulate generator faults.

Key words: generator; maintenance; diagnostic, marine; ship

1. INTRODUCTION

Modern autonomous electrical power systems on board marine vessels such as ships and offshore wind farms are becoming more complex. The onboard electrical energy is responsible for more and more mission-critical systems such as propulsion and stabilization. The safety and reliability of the marine system are determined by the electrical system's uninterrupted performance.

There are two main methods to ensure the uninterrupted performance of marine electrical autonomous power systems. The typical approach is preventative maintenance [1, 2], which has replaced the previously used corrective maintenance, that is, performing maintenance after a failure has occurred. Preventative maintenance is usually performed as time-based maintenance, where the equipment is checked within predetermined intervals. The main problem with such an approach is the increased number of scheduled maintenance procedures on equipment, which is essentially in good condition. Of course, this approach reduces the amount of downtime of mission-critical components at an increased cost of servicing.

A more modern approach, that is being introduced to and implemented in the maintenance of the marine system, is predictive maintenance [1, 2]. This also allows for a reduction in downtime of mission-critical components and allows for a reduction in the cost of servicing the vessel. One of the implementations of predictive maintenance is Condition Based Monitoring (CBM) [3] in combination with an automatic Decision Support System (DSS). In this approach, the selected system can be monitored for signs of upcoming failure and the decision system can automatically schedule the maintenance task.

The basis for the online diagnosis of the generator performance can be the Electrical Signature Analysis (ESA) or the Motor Current Signature Analysis (MCSA) techniques [4, 5, 6]. Those methods are based on comparing the amplitude and phase spectra of armature voltage and current waveforms with the spectra of a healthy generator. In MCSA, only stator (armature) current measurements are collected and processed to identify small changes in current signatures, eg. by harmonic analysis. The ESA method additionally uses the measurement of the stator (armature) voltage. It has been shown that, after appropriate treatment, ESA indicators are sensitive to mechanical and electrical disturbances occurring in engines and their driven devices. The MCSA and ESA were originally developed at the Oak Ridge National Laboratory for fault diagnosis of electric motors, and are now successfully applied to other types of electrical machinery and equipment. In simplified terms, the ESA method can be used as follows: based on the amplitude and phase change of certain harmonics it is possible to detect the Rotor Interturn Short Circuit (RISC), Stator Interturn Short Circuit (SICS), and other internal failures of the generator.

The consequence of using modern diagnostic methods is the possibility of fault-tolerant operation of the machine [7]. It is crucial to determine which failures would make the machine inoperable instantly and with which the generator can still operate. For example, the failure in the exciter discharge resistor would cause the machine to not be able to de-excite quickly which will increase the possibility of tripping the protection system when the generator load changes rapidly and causing blackout. However, this should not cause any danger of damaging the generator.

Proposed online detection methods usually rely either on additional components like special coils for measuring the presence of faults [8] or a model that allows for parallel computation and comparison with measured values [9]. The disadvantage of the second approach is the requirement for detailed model parameters of an undamaged generator. The main novelty of the paper is the development of a diagnostic algorithm that relies on existing protective equipment and requires mea-

*e-mail: filip.kutt@pg.edu.pl
**e-mail: michal.michna@pg.edu.pl
***e-mail: grzegorz.kostro@pg.edu.pl

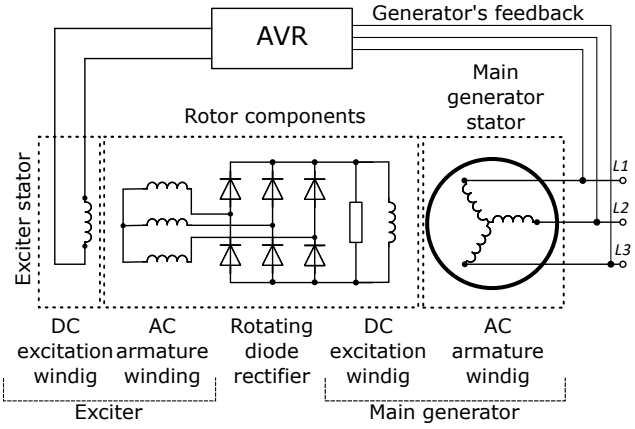

Fig. 1. Typical marine type brushless synchronous generator structure

surements of the BSG armature voltage spectrum. The following chapters describe, in Chapter 2, the typical BSG and its protective system components, in Chapter 3, failure modes of BSG and their detection algorithm are described and in Chapter 4, the simulations and measurements of selected failure modes are presented.

2. BRUSHLESS SYNCHRONOUS GENERATOR

2.1. Generator structure

The main source of electrical energy in marine power systems is the Brushless Synchronous Generator (BSG). The general structure of such a generator is shown in fig. 1. The BSG consists of two main components: the exciter and the main generator. The main generator field winding is supplied from the exciter armature via the rotating diode rectifier, usually a 3-phase full bridge. Because, of the complexity of this excitation supply circuit compared to the rest of the BSG components, failures of the excitation system are the most common failures of the BSG [8].

2.2. Generator protective equipment

The marine power system usually consists of several BSGs that operate on common busbars in parallel, so the protection equipment should reflect this. The typical protection equipment like over current, short circuit, under/over voltage and frequency is supplemented by additional reverse power control. Modern marine power generation systems also use a Power Management System (PMS) that measures power quality based on harmonic and THD of voltage and current waveforms at BSG output terminals. Typical components of the BSG protection equipment are shown in fig. 2.

3. FAILURE MODES DETECTION

Synchronous generator failure modes can be caused by external or internal sources. Some emergency states are effectively detected by the generator protection system. Therefore, it is important to select failure modes for diagnosis (other than those detected by a standard protection system), as well as to define methods of their diagnosis.

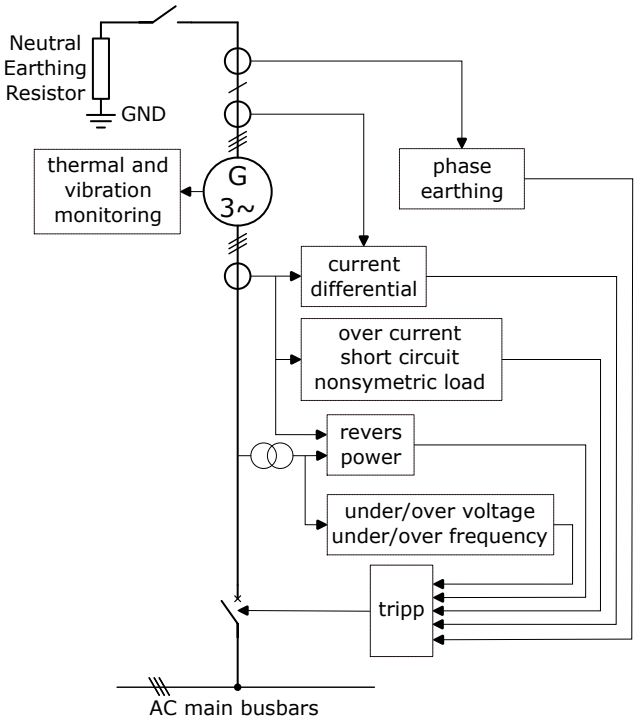

Fig. 2. Typical marine type brushless synchronous generator protective circuits

Table 1. Failure modes caused by external sources

Failure Modes (Tab. 3)	AVR failure	PS failure short-circuit	PS failure overload	PS perf. asymmetric load	PS perf. nonlinear load	Engine governor failure
UV	✓	✓	✓			
OV	✓					
VTHD					✓	
UF			✓			✓
OF						✓
OC			✓	✓		
ITHD					✓	
RP						✓
RC	✓					✓
EL		✓				
DIFF				✓		
MV				✓		✓
DE						

Typical failure modes for synchronous generators are listed below. Typical failure modes for synchronous generators caused by external sources are listed in Table 1 and by internal sources in Table 2. The failure mode codes are explained in Table 3. It should be noted that different causes can lead to the same failure modes.

3.1. Main generator excitation winding failure

Main generator excitation winding failure can be caused by:

Table 2. Failure modes caused by internal sources

Failure Modes (Tab. 3)	Main gen. excitation wind. failure	Main gen. armature wind. failure	Exciter excitation winding failure	Exciter armature winding failure	Exciter diode rectifier failure	Static rotor eccentricity	Dynamic rotor eccentricity	Inter-laminar core fault
UV	✓	✓	✓	✓	✓			
OV								
VTHD	✓	✓			✓		✓	
UF								
OF								
OC								
ITHD		✓					✓	
RP								
RC								
EL	✓	✓	✓	✓				
DIFF		✓				✓		
MV	✓	✓					✓	
DE								✓

- Turn-to-turn short circuit in excitation winding
- Open circuit in excitation winding
- Grounding of the excitation winding

The excitation winding open circuit causes immediate UV protection trip and the grounding of the excitation winding might not be detectable until the presence of a second grounding fault in the excitation winding. In a such case, the machine will behave as with the turn-to-turn short circuit in excitation winding.

Turn-to-turn failure of the excitation winding causes the AVR to increase the excitation current up to the limit after which the undervoltage operation will occur. This can be indicated by the change in the transfer characteristic of the generator k_{tr}:

$$k_{tr} = \frac{U_{RMS}}{I_e} \tag{1}$$

where U_{RMS} is the generator armature voltage and I_e is the exciter excitation current. This value in a healthy generator operating in no-load conditions at the nominal armature voltage should be constant, in other words, the same value of excitation current will induce the same armature voltage at the same rotational velocity. If there is a rotor winding inter-turn short circuit present then this constant will decrease.

The armature voltage/current spectrum components that can (not always) exhibit a change during the rotor fault are the components caused by the mechanical rotation of the machine [4]:

$$f_{erh} = f_e \pm k \cdot f_r \tag{2}$$

where $k \in N$, f_e is the fundamental component of the armature electrical frequency, f_{erh} are the armature voltage spectrum components in question, and the f_r is the mechanical frequency of the rotor and is equal to:

$$f_r = \frac{f_e}{p} \tag{3}$$

where p is the number of pole pairs of the generator. The mechanical vibration will occur due to the unbalanced air gap flux of the machine and due to uneven temperature distribution in the rotor [10].

In addition to the armature voltage/current spectrum components caused by mechanical rotation the even armature voltage/current harmonic components also can manifest themself during rotor excitation winding fault [4, 11]:

$$f_{eh} = f_1 + (2k-1) \cdot f_1 \tag{4}$$

where $k \in N$ and f_{eh} are the even armature voltage/current harmonics.

3.2. Main generator armature winding failure

Main generator armature winding failure can be caused by:

- Turn-to-turn short circuit in the armature winding
- Phase-to-phase short circuit in the armature winding
- Open circuit in the armature winding
- Grounding of the armature winding

Turn-to-turn short circuit in the armature winding can manifest themselves with armature voltage asymmetry caused by the decrease of effective coil turns of one of the armature windings. Also in the shorted part of the winding, the pulsating current creates a pulsating magnetic field. This magnetic field can manifest itself in armature voltage/current waveforms as a third harmonic.

Phase-to-phase short circuit in the armature winding can manifest themselves with high armature voltage asymmetry, a rapid increase in temperature, and a high increase in machine vibration.

An open circuit in the armature winding manifests itself with a high asymmetry of the armature voltage (one or more phase voltages are not present)

Grounding of the armature winding can be detected both by the earth leakage EL protection and by the differential current DIFF protection. In the HV system in case of single-phase grounding, a high current will flow through the Neutral Earthing Resistor (NER) causing a generator protection trip.

3.3. Exciter excitation winding failure

Exciter excitation winding failure can be caused by:

- Turn-to-turn short circuit in excitation winding
- Open circuit in excitation winding
- Grounding of the excitation winding

Turn-to-turn short circuit in the exciter excitation winding will manifest itself by the change transfer characteristic of the generator k_{tr} as with the main generator excitation winding. The unbalanced air gap magnetic flux distribution will be present. Because of the relatively low power of the exciter the vibration caused by the unbalance might not be detectable.

Open circuit in excitation winding will manifest itself by the error in AVR operation and the lack of machine armature voltage (armature voltage below 40%). The AVR will not output any current whatsoever.

Grounding of the excitation winding might not be detectable until the presence of a second grounding fault in the excitation winding. In a such case, the machine will behave as with the turn-to-turn short circuit in excitation winding.

3.4. Exciter armature winding failure

Exciter armature winding failure can be caused by:

- Turn-to-turn short circuit in the exciter armature winding
- Phase-to-phase short circuit in the exciter armature winding
- Open circuit in the exciter armature winding
- Grounding of the armature winding

Turn-to-turn short circuit in the exciter armature winding can manifest itself with exciter armature voltage asymmetry. This asymmetry will influence the excitation current waveform. The armature voltage/current spectrum components will correspond with the harmonic components of the exciter armature voltage/current. The fundamental component of this spectrum is defined by the machine rotational velocity and the number of pole pairs of the machine exciter.

As with the generator armature winding also in the shorted part of the winding, the pulsating current creates a pulsating magnetic field. This magnetic field can manifest itself in the excitation current of the exciter as a waveform spectrum component:

$$f_{exf} = 3 \cdot f_{ex} \tag{5}$$

where f_{ex} is the nominal frequency of the exciter armature voltage and f_{exf} is the frequency of the exciter field spectrum component.

Phase-to-phase short circuit in the exciter armature winding will cause high asymmetry in the armature voltage. This will manifest itself with pulsation excitation (component with the frequency of f_{ex}) current and the main generator spectrum components as described in the next section concerning the operation with the damaged diode bridge rectifier.

An open circuit in the exciter armature winding will cause high asymmetry in the armature voltage. This will manifest itself with pulsation excitation (component with the frequency of f_{ex}) current and the main generator spectrum components as described in the next section concerning the operation with the damaged diode bridge rectifier. The performance will be a simulator to open diode performance.

Grounding of the armature winding as with the excitation winding single earth leakage will not be detectable. In case of at least two ground faults, the behavior will be similar to a turn-to-turn or phase-to-phase short circuit depending on the grounded phases.

3.5. Exciter diode rectifier failure

Exciter diode rectifier failure can be caused by a short-circuit or interrupted diode. Typical diode failures, whether short circuit or open circuit, are preceded by a period of increasing reverse leakage current in the device [12].

Compensating leakage current requires increasing the rectifier voltage, which is observed by the increased exciter excitation current. As a result, the Brushless Transfer Characteristic changes, similar to the short-circuit of the main field turns. An exciter diode rectifier faults can be also diagnosed based on the harmonic armature voltage analysis. This damage usually leads to a reduction in the excitation current and the appearance of UV mode.

A symptom of this type of fault is the appearance of characteristic frequency in the induced voltage spectrum [13, 14]. The value of this frequency can be calculated from the equation:

$$\begin{aligned} f^{-}_{(1:1)} &= (p_e - p) \cdot \omega_r \\ f^{+}_{(1:1)} &= (p_e + p) \cdot \omega_r \end{aligned} \tag{6}$$

where:

p_e - number of pair poles of an exciter
p_m - number of pair poles of a main generator
ω_r - rotating velocity of a main generator in [1/s]
$f^{-}_{(1:1)}, f^{+}_{(1:1)}$ - frequencies characteristic for failure in a rectifier bridge

An interrupted diode can be distinguished from a short circuit by analyzing the quotient of harmonic amplitudes $f^{-}_{(1:1)}$ i $f^{+}_{(1:1)}$. If:

$$\frac{E^{+}_{(1:1)}}{E^{-}_{(1:1)}} = \frac{f^{+}_{(1:1)}}{f^{-}_{(1:1)}} \tag{7}$$

then there is a break in the branch of the rotating rectifier bridge, while if:

$$\frac{E^{+}_{(1:1)}}{E^{-}_{(1:1)}} \ll \frac{f^{+}_{(1:1)}}{f^{-}_{(1:1)}} \tag{8}$$

then the fault is a short-circuit in the branch of the rotating rectifier bridge; where:

$E^{-}_{(1:1)}, E^{+}_{(1:1)}$ - amplitudes of the characteristic harmonics
$f^{-}_{(1:1)}, f^{+}_{(1:1)}$ - frequencies characteristic for failure in a rectifier bridge.

The proposed procedure for detecting this damage should be based on the observation of changes in the Brushless Transfer Characteristic and additional harmonic analysis of armature currents and voltages.

3.6. Rotor eccentricity

The rotor eccentricity can be caused by mechanical or electrical damage. Mechanical damage is the most common cause of failure of electrical machines. About 60% of these faults are caused by damage of the mechanical parts such as bearings and shafts. As a consequence, mechanical damage leads to a shift in the axis of symmetry of the axis of symmetry or the rotating axis of the rotor [15]. There are two types of rotor eccentricity: the static and the dynamic asymmetry.

Static asymmetry is characterized by the fact that the position of the maximum air gap on the circumference of the machine is constant. Static asymmetry may result from the ovality of the rotor or stator core, incorrect assembly, or one-sided magnetic tension. Dynamic rotor asymmetry is characterized by the fact that the position of the maximum air gap changes with the position of the rotor. Dynamic asymmetry may result from wear of bearing, or a bent shaft, and is most often caused by wear of the machine during its operation [15].

This damage will manifest as unbalanced radial forces (unbalanced magnetic pull or UMP) and consequently, an increase in vibration and noise levels. A rotor eccentricity of up to 10% is allowed. However, to reduce vibration and noise, it is recommended to keep it at a lower level. Damage detection may be based on the analysis of signals from the drag sensor or the frequency analysis of the armature voltage or current waveforms [16]. Vibration signals can be monitored to detect eccentricity-related faults. The high-frequency vibration components for static or dynamic eccentricity are given by:

$$f_v = 2f \pm f_r \tag{9}$$

However, the vibration signature analysis has several disadvantages. It requires at least one vibration sensor and additional costs related to its proper installation and maintenance. The interpretation of the results requires machine-dependent information and expert involvement.

Accordingly, alternative diagnostic methods based on MCSA and ESA are being developed. Due to the vibrations of the rotor, an alternating component appears in the excitation voltage and current, which in turn can be observed in the form of additional harmonics in the armature currents and voltages. In the case of the analyzed generator, with brushless excitation, a significant limitation is the lack of access to the excitation current. The analysis of additional harmonics of the current and armature voltage requires information on the structure of the machine, including winding distribution.

In the event of asymmetry, additional harmonics can be observed in the waveform of the armature current. Frequency of additional harmonics [17]:

$$\begin{aligned} f_{k1} &= kf_1 - \frac{(p-1)f_1}{p} \\ f_{k2} &= 2kf_1 \end{aligned} \tag{10}$$

where: f_{k1} , f_{k2} – Frequency of additional current harmonics, p – number of pole pairs, f_1 – frequency of fundamental harmonic, k – natural number, eccentricity order

The simulation presented in [18] results show that the 17th and 19th harmonics can be employed to diagnose the dynamic eccentricity of the machine. The results of the analyses presented in the literature confirm that it is possible to diagnose the eccentricity of the rotor based on the current and voltage signature analysis and the observation of harmonic components of the 2f order [16, 19, 20, 21].

3.7. Inter-laminar core fault

An inter-laminar fault is occurring in the armature of the main generator. Detection of inter-laminar short circuit fault is difficult. The method presented in the literature required special probes (ELectromagnetic Core Implementation Detector – EL CID) [22, 23, 24, 25], or additional windings [26] and removal of the rotor during tests. Therefore detection of this kind of fault is performed during manufacturing or repairing the generator.

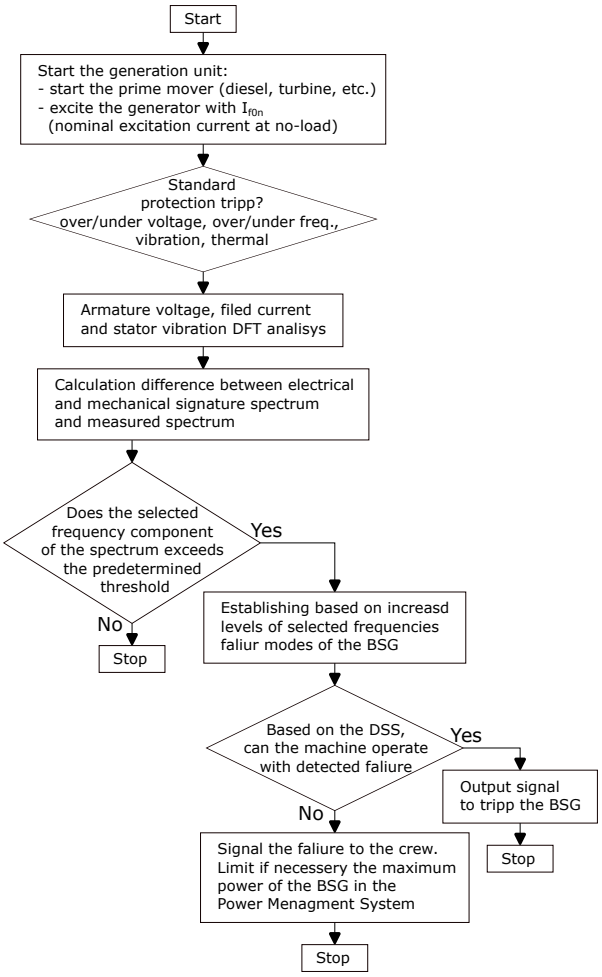

Fig. 3. Failure detection algorithm

3.8. Failure detection algorithm

Based on the analysis of different failure modes a general algorithm that can be implemented in the existing BSG protection system was developed. Fig. 3 shows the proposed algorithm.

4. SIMULATIONS AND MEASUREMENTS

Simulations and measurements were conducted using a standard electromagnetically excited slip-ring synchronous generator without internal exciter. The nominal parameters of the synchronous generator type ELMOR GCe64a are:

- Output power 10 kVA
- Rated voltage: 231 V
- Rated current: 25 A
- Power factor: 0.8
- Frequency 50 Hz

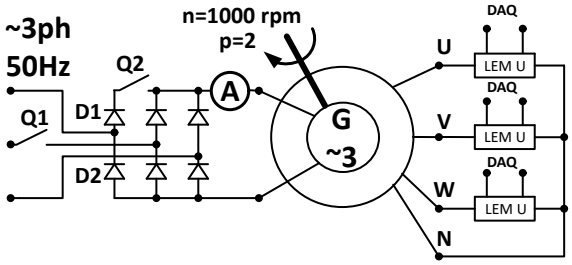

Fig. 4. Measurement diagram for generator no-load test

- Rated speed 1500 rpm

The exciter of the generator was emulated using a 3-phase auto-transformer and full bridge diode rectifier supplying the excitation of the main generator through the slip rings. The measurements were conducted at the LINTE^2 laboratory test bench of the Gdansk University of Technology. The following generator operating states were emulated:

- undamaged system,
- disconnection/failure of the rotating rectifier diode – described in section 3.5,
- disconnection/failure of the exciter armature phase (failure of two diodes in one arm of a rotation bridge rectifier) – described in section 3.4.

Measurements of all three operating states were made both in no-load (Fig. 4) and short-circuit conditions. However, for further analysis, only the no-load test will be considered, as this can be easily performed during normal operation of the power system (just before the generator is synchronized and connected to the main switchboard).

The GCe64a generator used in tests has 4 poles. During tests, rotation speed was equal to 1000 rpm and the rectifier in the excitation circuit was fed from a three-phase source with a frequency equal to 50Hz. This test configuration emulates a typical marine system where the exciter is a 6-pole generator and the main generator has 4 poles. Therefore, the nominal frequency of the main generator is equal to 33.33 Hz. It was expected that in this case, an open circuit in the rectifier bridge caused the harmonics in the measured signals with a frequency equal to:

$$\begin{aligned} f^{-}_{(1:1)} &= (p_e - p) \cdot 16.67 = 16.67 \text{ Hz} \\ f^{+}_{(1:1)} &= (p_e + p) \cdot 16.67 = 83.35 \text{ Hz} \end{aligned} \tag{11}$$

Measurements were recorded using a measurement National Instruments DAQ USB-6251 with a 16-bit, 1.25 MS/s AD converter and controlled by DAQExpress software.

Simulations were performed in Synopsys Saber simulation software using a synchronous generator (SG) model developed based on the [27]. The model and simulation parameters were determined based on the data of the generator used during the laboratory measurements. Two SG models were connected together to form the exciter and main generator system with a full bridge rectifier between them. Fig. 6 shows the schematic of the simulation circuit in Synopsys Saber.

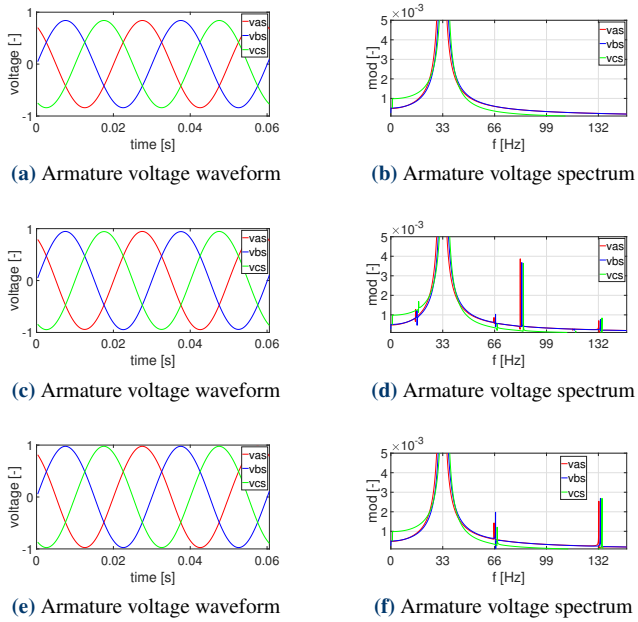

(a) Armature voltage waveform (b) Armature voltage spectrum

(c) Armature voltage waveform (d) Armature voltage spectrum

(e) Armature voltage waveform (f) Armature voltage spectrum

Fig. 5. Simulations of (a,b) undamaged system, (c,d) single diode failure - D1, (e,f) dual diode failure - D1 and D2.

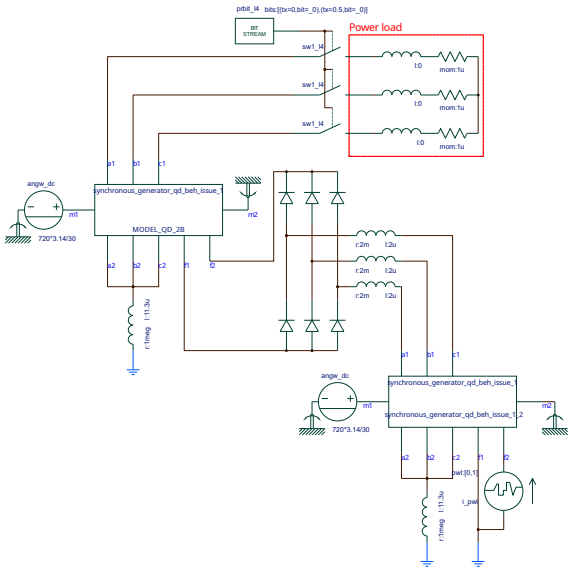

Fig. 6. Simulation model circuit diagram for generator no-load test

The model was developed using main voltage equations based on the SG model in an orthogonal $qd0$ reference frame and is defined as:

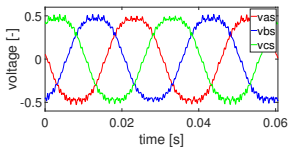

(a) Armature voltage waveform

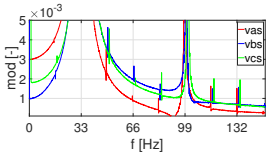

(b) Armature voltage spectrum

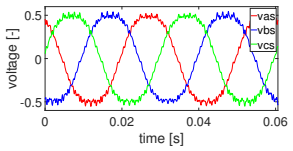

(c) Armature voltage waveform

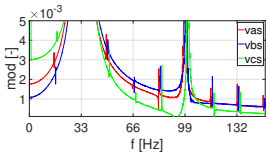

(d) Armature voltage spectrum

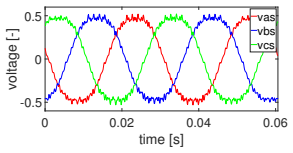

(e) Armature voltage waveform

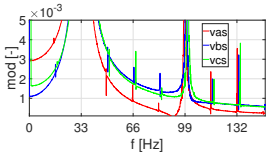

(f) Armature voltage spectrum

Fig. 7. Measurements of (a,b) undamaged system, (c,d) single diode failure - D1, (e,f) dual diode failure - D1 and D2.

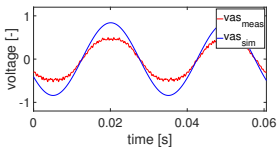

(a) Armature voltage waveform

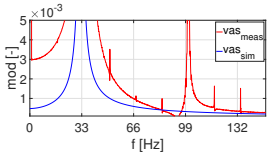

(b) Armature voltage spectrum

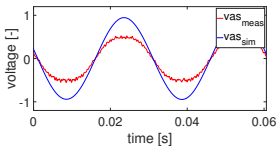

(c) Armature voltage waveform

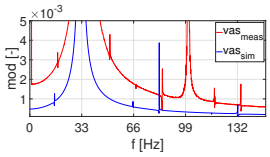

(d) Armature voltage spectrum

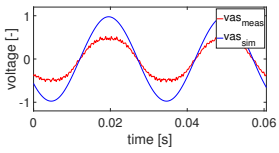

(e) Armature voltage waveform

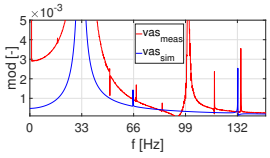

(f) Armature voltage spectrum

Fig. 8. Measurements (meas) and simulations (sim) of (a,b) undamaged system, (c,d) single diode failure - D1, (e,f) dual diode failure - D1 and D2.

$$v_{qs}^{r} = -r_s i_{qs}^{r} + \omega_r \lambda_{ds}^{r} + \frac{\mathrm{d}\lambda_{qs}^{r}}{\mathrm{d}t} \tag{12}$$

$$v_{ds}^{r} = -r_s i_{ds}^{r} - \omega_r \lambda_{qs}^{r} + \frac{\mathrm{d}\lambda_{ds}^{r}}{\mathrm{d}t} \tag{13}$$

$$v_{0s}^{r} = -r_s i_{0s}^{r} + \frac{\mathrm{d}\lambda_{0s}^{r}}{\mathrm{d}t} \tag{14}$$

$$0 = r_{kq}' i_{kq}'^{r} + \frac{\mathrm{d}\lambda_{kq}'^{r}}{\mathrm{d}t} \tag{15}$$

$$0 = r_{kd}' i_{kd}'^{r} + \frac{\mathrm{d}\lambda_{kd}'^{r}}{\mathrm{d}t} \tag{16}$$

$$v_{fd}'^{r} = r_{fd}' i_{fd}'^{r} + \frac{\mathrm{d}\lambda_{fd}'^{r}}{\mathrm{d}t} \tag{17}$$

In both the simulations and measurements three different performances were analyzed:

- Normal healthy operation of the system
- Single rotating rectifier bridge diode failure – diode D1 disconnected
- Dual diode bridge rectifier failure – diode D1 and D2 disconnected, emulation exciter phase failure or short circuit in the rectifier

Results are presented fig. 5 in relative units related to the nominal amplitude of generator armature voltage. In the no-load test, the analysis is based on the results of the amplitude spectrum of the armature voltage.

Performed simulations and measurements are compared and shown in fig. 8.

Even for the undamaged generator, the no-load voltage spectrum contains a lot of spectrum components (fig. 7). This high THD value (>5%) is characteristic of the GCe64a type generator design. The amplitude of spectrum components with frequencies $f_{(1:1)}^{-}$=16.6Hz and $f_{(1:1)}^{+}$=83.35Hz increase when single diode failure is emulated. For dual diode failure mode (exciter phase failure), the amplitude of the second (66Hz) and fourth (132Hz) harmonic (of the generator armature voltage/current fundamental component) increases compared to the undamaged generator. The amplitude changes are approximately 0.1% of the fundamental harmonic. Performed simulations and measurements are compared and shown in fig. 8 in order to illustrate those changes.

5. CONCLUSIONS

Presented simulation and measurement results show that the ESA method is a viable solution for diagnostic system development. However, the changes in spectrum components between the healthy and damaged generator are three orders of magnitude lower than the fundamental component (0.1%). During the measurements, a 16-bit ADC (analog digital converter) was used. This allows for 0.001% accuracy. The implementation of such a system can rely on filtering and amplifying characteristic frequencies in order to improve such system performance. The no-load test can be performed when the generator is starting and just before the generator goes offline.

During the on line performance of the generator different approach would have to be applied. The ESA should be performed on a healthy generator while on load and compared with the generator continuously. However, in the typical marine system, there are multiple nonlinear loads that can introduce certain harmonic frequencies so a more comprehensive analysis should be performed. The transfer characteristic 1 and the harmonic components should be compared to the signature of the healthy generator to eliminate the influence of other marine power system components on the BSG performance.

Table 3. Failure modes acronyms

Failure Modes	Acronym
Undervoltage operation	UV
Overvoltage operation	OV
Voltage THD increase	VTHD
Under frequency operation	UF
Over frequency operation	OF
Overcurrent operation	OC
Current THD increase	ITHD
Revers power operation	RP
Reverse current operation	RC
Earth leakage Low Insulation state	EL
Electric asymmetry current differential	DIFF
Mechanical vibration	MV
Decreased efficiency increased torque	DE
Power system	PS

APPENDIX

Tab. 3 list the acronyms used in Tab. 2 and Tab. 1.

REFERENCES

[1] A. A. Daya and I. Lazakis, "Developing an advanced reliability analysis framework for marine systems operations and maintenance," Ocean Engineering, vol. 272, p. 113766, mar 2023.

[2] Ç. Karatuğ, Y. Arslanoğlu, and C. G. Soares, "Review of maintenance strategies for ship machinery systems," Journal of Marine Engineering & Technology, vol. 22, no. 5, pp. 233–247, sep 2023. [Online]. Available: https://www.tandfonline.com/doi/abs/10.1080/20464177.2023.2180831

[3] A. L. Michala, I. Lazakis, and G. Theotokatos, "Predictive maintenance decision support system for enhanced energy efficiency of ship machinery," nov 2015. [Online]. Available: https://eprints.gla.ac.uk/138014/

[4] C. P. Salomon, C. Ferreira, W. C. Sant'Ana, G. Lambert-Torres, L. E. Borges da Silva, E. L. Bonaldi, L. E. d. L. de Oliveira, and B. S. Torres, "A Study of Fault Diagnosis Based on Electrical Signature Analysis for Synchronous Generators Predictive Maintenance in Bulk Electric Systems," Energies, vol. 12, no. 8, p. 1506, apr 2019. [Online]. Available: https://www.mdpi.com/1996-1073/12/8/1506

[5] C. P. Salomon, W. C. Santana, E. L. Bonaldi, L. E. L. de Oliveira, L. E. Borges da Silva, J. G. Borges da Silva, G. Lambert-Torres, A. Pellicel, M. A. A. Lopes, and G. C. Figueiredo, "A study of electrical signature analysis for two-pole synchronous generators," in 2017 IEEE International Instrumentation and Measurement Technology Conference (I2MTC). IEEE, may 2017, pp. 1–6. [Online]. Available: http://ieeexplore.ieee.org/document/7969795/

[6] N. Bessous, S. Sbaa, and A. Megherbi, "Mechanical fault detection in rotating electrical machines using mcsa-fft and mcsa-dwt techniques," Bulletin of the Polish Academy of Sciences Technical Sciences, vol. 67, no. No. 3, pp. 571–582, 2019. [Online]. Available: http://journals.pan.pl/Content/113169/PDF/14_571-582_01009_Bpast.No.67-3_06.02.20.pdf

[7] T. I. Bo and T. A. Johansen, "Scenario-based fault-tolerant model predictive control for diesel-electric marine power plant," OCEANS 2013 MTS/IEEE Bergen: The Challenges of the Northern Dimension, 2013.

[8] Y. Wu, B. Cai, and Q. Ma, "An Online Diagnostic Method for Rotary Diode Open-Circuit Faults in Brushless Exciters," IEEE Transactions on Energy Conversion, vol. 33, no. 4, pp. 1677–1685, dec 2018.

[9] K. Mahtani, J. M. Guerrero, L. F. Beites, and C. A. Platero, "Application of a Model-Based Method to the Online Detection of Rotating Rectifier Faults in Brushless Synchronous Machines," Machines 2023, Vol. 11, Page 223, vol. 11, no. 2, p. 223, feb 2023. [Online]. Available: https://www.mdpi.com/2075-1702/11/2/223/htmhttps://www.mdpi.com/2075-1702/11/2/223

[10] "C37.102-2023 - IEEE Guide for AC Generator Protection," 2024.

[11] W. Yucai and L. Yonggang, "Diagnosis of Rotor Winding Interturn Short-Circuit in Turbine Generators Using Virtual Power," IEEE Transactions on Energy Conversion, vol. 30, no. 1, pp. 183–188, mar 2015. [Online]. Available: http://ieeexplore.ieee.org/document/6871347/

[12] T. D. Batzel and D. C. Swanson, "Prognostic Health Management of Aircraft Power Generators," IEEE Transactions on Aerospace and Electronic Systems, vol. 45, no. 2, pp. 473–482, apr 2009. [Online]. Available: http://ieeexplore.ieee.org/document/5089535/

[13] M. Salah, K. Bacha, A. Chaari, and M. E. H. Benbouzid, "Brushless Three-Phase Synchronous Generator Under Rotating Diode Failure Conditions," IEEE Transactions on Energy Conversion, vol. 29, no. 3, pp. 594–601, sep 2014. [Online]. Available: http://ieeexplore.ieee.org/document/6785994/

[14] M. Rahnama and A. Vahedi, "Rotary diode failure detection in brushless exciter system of power plant synchronous generator," in 2016 6th Conference on Thermal Power Plants (CTPP). IEEE, jan 2016, pp. 6–11. [Online]. Available: http://ieeexplore.ieee.org/document/7482926/

[15] S. Nandi, H. Toliyat, and X. Li, "Condition Monitoring and Fault Diagnosis of Electrical Motors—A Review," IEEE Transactions on Energy Conversion, vol. 20, no. 4, pp. 719–729, dec 2005. [Online]. Available: http://ieeexplore.ieee.org/document/1546063/

[16] G. Joksimovic, C. Bruzzese, and E. Santini, "Static eccentricity detection in synchronous generators by field current and stator Voltage Signature Analysis - Part I: Theory," in The XIX International Conference on Electrical Machines - ICEM 2010. IEEE, sep 2010,

pp. 1–6. [Online]. Available: http://ieeexplore.ieee.org/document/5607945/

[17] M. Baranski, "New vibration diagnostic method of PM generators and traction motors - Detecting of vibrations caused by unbalance," ENERGYCON 2014 - IEEE International Energy Conference, pp. 28–32, 2014.

[18] I. Tabatabaei, J. Faiz, H. Lesani, and M. T. Nabavi-Razavi, "Modeling and simulation of a salient-pole synchronous generator with dynamic eccentricity using modified winding function theory," IEEE Transactions on Magnetics, vol. 40, no. 3, pp. 1550–1555, 2004.

[19] C. Bruzzese, A. Giordani, and E. Santini, "Static and Dynamic Rotor Eccentricity On-Line Detection and Discrimination in Synchronous Generators By No-Load E.M.F. Space Vector Loci Analysis," in 2008 International Symposium on Power Electronics, Electrical Drives, Automation and Motion. IEEE, jun 2008, pp. 1259–1264. [Online]. Available: https://ieeexplore.ieee.org/document/4581180/

[20] C. Bruzzese, E. Santini, V. Benucci, and A. Millerani, "Model-based eccentricity diagnosis for a ship brushless-generator exploiting the Machine Voltage Signature Analysis (MVSA)," in 2009 IEEE International Symposium on Diagnostics for Electric Machines, Power Electronics and Drives. IEEE, aug 2009, pp. 1–7. [Online]. Available: http://ieeexplore.ieee.org/document/5292763/

[21] C. Bruzzese, A. Giordani, A. Rossi, and E. Santini, "Synchronous Generator Eccentricities Modeling by Improved MWFA and Fault Signature Evaluation in No-Load E.M.F.s and Current Spectra," in 2008 International Symposium on Power Electronics, Electrical Drives, Automation and Motion. IEEE, jun 2008, pp. 200–205. [Online]. Available: https://ieeexplore.ieee.org/document/4581181/

[22] S. Lee, G. Kliman, M. Shah, N. Nair, and R. Lusted, "An Iron Core Probe Based Inter-Laminar Core Fault Detection Technique for Generator Stator Cores," IEEE Transactions on Energy Conversion, vol. 20, no. 2, pp. 344–351, jun 2005. [Online]. Available: http://ieeexplore.ieee.org/document/1432847/

[23] R. Romary, C. Demian, P. Schlupp, and J.-Y. Roger, "Offline and Online Methods for Stator Core Fault Detection in Large Generators," IEEE Transactions on Industrial Electronics, vol. 60, no. 9, pp. 4084–4092, sep 2013. [Online]. Available: http://ieeexplore.ieee.org/document/6329432/

[24] H. Hamzehbahmani, P. Anderson, and K. Jenkins, "Interlaminar Insulation Faults Detection and Quality Assessment of Magnetic Cores Using Flux Injection Probe," IEEE Transactions on Power Delivery, vol. 30, no. 5, pp. 2205–2214, 2015.

[25] D. Bertenshaw, A. Smith, C. Ho, T. Chan, and M. Sasic, "Detection of stator core faults in large electrical machines," IET Electric Power Applications, vol. 6, no. 6, p. 295, 2012. [Online]. Available: https://digital-library.theiet.org/content/journals/10.1049/iet-epa.2011.0125

[26] S. Lee, G. Kliman, M. Shah, W. Mall, N. Nair, and R. Lusted, "An Advanced Technique for Detecting Inter-Laminar Stator Core Faults in Large Electric Machines," IEEE Transactions on Industry Applications, vol. 41, no. 5, pp. 1185–1193, sep 2005. [Online]. Available: http://ieeexplore.ieee.org/document/1510816/

[27] S. P. Paul Krause, Oleg Wasynczuk, Scott Sudhoff, Analysis of Electric Machinery and Drive Systems, P. Krause, O. Wasynczuk, S. Sudhoff, and S. Pekarek, Eds. Wiley, jun 2013. [Online]. Available: https://onlinelibrary.wiley.com/doi/book/10.1002/9781118524336